

Available online at www.sciencedirect.com

ScienceDirect

www.elsevier.com/locate/jes

JES
 JOURNAL OF
 ENVIRONMENTAL
 SCIENCES
www.jesc.ac.cn

Functional groups assisted-photoinduced electron transfer-mediated highly fluorescent metal-organic framework quantum dot composite for selective detection of mercury (II) in water

Karanika Sonowal^{1,2}, Lakshi Saikia^{1,2,*}

¹Advanced Materials Group, Materials Sciences and Technology Division, CSIR-North East Institute of Science and Technology, Jorhat, Assam 785006, India

²Academy of Scientific and Innovative Research (AcSIR), Ghaziabad 201002, India

ARTICLE INFO

Article history:

Received 22 February 2022

Revised 19 May 2022

Accepted 20 May 2022

Available online 30 May 2022

Keywords:

Binary metal-organic framework composite (NH₂-UiO-66/g-CNQDs)
 Graphitic carbon nitride quantum dots (g-CNQDs)

Fluorescence sensing

Mercury (II) detection

Aqueous medium

ABSTRACT

The presence of toxic mercury (II) in water is an ever-growing problem on earth that has various harmful effect on human health and aquatic living organisms. Therefore, detection of mercury (II) in water is very much crucial and several researches are going on in this topic. Metal-organic frameworks (MOFs) are considered as an effective device for sensing of toxic heavy metal ions in water. The tunable functionalities with large surface area of highly semiconducting MOFs enhance its activity towards fluorescence sensing. In this study, we are reporting one highly selective and sensitive luminescent sensor for the detection of mercury (II) in water. A series of binary MOF composites were synthesized using in-situ solvothermal synthetic technique for fluorescence sensing of Hg²⁺ in water. The well-distributed graphitic carbon nitride quantum dots on porous zirconium-based MOF improve Hg²⁺ sensing activity in water owing to their great electronic and optical properties. The binary MOF composite (2) i.e., the sensor exhibited excellent limit of detection (LOD) value of 2.4 nmol/L for Hg²⁺. The sensor also exhibited excellent performance for mercury (II) detection in real water samples. The characterizations of the synthesized materials were done using various spectroscopic techniques and the fluorescence sensing mechanism was studied.

© 2022 The Research Center for Eco-Environmental Sciences, Chinese Academy of Sciences. Published by Elsevier B.V.

Introduction

Rapid industrialization is causing over exposure to mercury (II) level on earth leading to health hazards for human beings due to the consumption of mercury contaminated foods. As mercury (II) is one of the toxic heavy metal ions, mainly

found in water and living aquatic lives and it comes to human body indirectly by consumption of living aquatic foods. Mercury ingestion can cause nausea, severe abdominal pain, renal damage, kidney problem, neurological disorder etc. Therefore, Hg²⁺ detection in water is very crucial to protect human health as well as environment. There are various techniques such as atomic absorption spectroscopy (AAS), inductively coupled plasma-mass spectroscopy (ICP-MS), colorimetric analysis etc. for Hg²⁺ detection. Though these are very helpful techniques, they have some limitations

* Corresponding author.

E-mail: lsaikia@neist.res.in (L. Saikia).

like high time consumption, sophisticated instrumentation, pre-sample preparation methods. Now-a-days, fluorescence-based method has been considered as an effective measure for Hg^{2+} detection in aqueous medium with less time consumption.

Among the ongoing research for mercury (II) detection in water, metal-organic frameworks (MOFs) are considered as effective devices to be used as sensor for this purpose. As we all know, MOFs are a class of highly porous three-dimensional polymeric materials consist of metal ions or small discrete clusters connected via multidentate organic spacers. The large surface area and tunability of functionalized MOFs enhance their activity in variety of applications such as gas storage, separation, catalysis, sensing, energy storage and conversion etc. (Chen et al., 2019; Gustafsson et al., 2010; Li et al., 2017; Liu et al., 2020; Luo et al., 2017; Ma, 2009; Shen et al., 2013; Silva et al., 2010; Tang et al., 2013; Wang et al., 2017b, 2021; Wu et al., 2017, 2019; Zhang et al., 2020, 2021). MOFs act as promising luminescent materials due to the presence of both organic and inorganic groups in the framework structure that makes them excellent probes towards sensing applications (Fang et al., 2018). The interesting factor of MOFs is their large porosities that allow guest species to diffuse into their bulk structures. Several research on sensing applications using semiconducting MOFs based sensors are still going on and many MOFs sensors for sensing of toxic metal ions have been reported till now (Li et al., 2016; Wang et al., 2017a; Xia et al., 2016; Zhao et al., 2015; Zhou et al., 2013b). Also, various MOFs composites as sensors containing traditional quantum dots such as CdS, CdSe, ZnO etc. have been reported so far for many sensing applications (Jin et al., 2017; Zhao et al., 2014). But the traditional quantum dots containing heavy metal ions have harmful effects on human health and environment due to their highly toxic nature (Aguilera-Sigalat and Bradshaw, 2016; Mirnajafizadeh et al., 2019). The fast electron-hole pair recombination of traditional quantum dots is another drawback which limits their applications to some extents. Therefore, it is very challenging to design highly luminescent functional MOFs with non-toxicity and improved functionality for mercury (II) detection in water. From literature, it is also found that many sensors are not stable in water. Therefore, architect of highly water stable MOFs based sensors are highly appreciable, also using water as reaction medium in place of costly, harmful organic solvents for sensing applications is highly demanded. In recent years, graphitic carbon nitride quantum dots (g-CNQDs) as metal-free polymeric materials with non-toxicity, good stability, good water solubility are gaining more importance in various fields including sensing of heavy metal ions rather than using traditional quantum dots (Zhou et al., 2013a; Zhu et al., 2014). g-CNQDs have high electron contents due to the presence of charge efficient functionalized surface groups (like -OH, -COO⁻) which leads to excellent electron carriage properties in exposure to light. Therefore, g-CNQDs can be considered as potential applicants for designing MOFs based sensors with enhanced chemical and electronic properties and to be used in sensing applications.

Among the various reported MOFs, NH_2 -UiO-66 is one of the most potential MOFs introduced by Karl Petter Lillerud and his co-workers. They first reported highly robust UiO-66 MOF

and demonstrated the possibility of modification by functionalization without losing its tremendous chemical and thermal stability (Kandiah et al., 2010a). They confirmed the morphology of UiO-66 and found that UiO-66 consists of a $\text{Zr}_6\text{O}_4(\text{OH})_4$ octahedra core which forms $\text{Zr}_6\text{O}_4(\text{OH})_4(\text{CO}_2)_{12}$ clusters. They further confirmed the amino functionalization of UiO-66 leading to NH_2 -UiO-66 and mentioned its chemical availability. Mats Tilsted and co-workers did the post-synthetic modifications of UiO-66 MOF due to its large surface area, high porosity, crystallinity, stability and presence of amino groups leading to various applications in gas adsorption, sensor, catalysis etc. (Kandiah et al., 2010b). Many research works are still going on various applications using NH_2 -UiO-66 MOF with lots of modifications (Wang et al., 2017a; Yu et al., 2019; Zhang et al., 2018). There are many Hg^{2+} sensing applications have been reported previously using MOFs and other materials (Chen et al., 2018; Deng et al., 2018; Liu et al., 2017; Wang et al., 2018c, 2018b; Xia et al., 2016). Some reports on mercury (II) detection in water based on fluorescence sensing method have been shown in Appendix A Table S1.

In this work, a binary MOF composite series of NH_2 -UiO-66/g-CNQDs were synthesized with good chemical and electronic stability. The binary MOF composite exhibited excellent electron rich properties and good fluorescence emission properties. The synthesized binary MOF composite has been used for fluorescence sensing of mercury (II) in water and a relative fluorescence sensing study for mercury (II) detection in water has been performed in between the synthesized NH_2 -UiO-66 MOF and binary MOF composite, NH_2 -UiO-66/g-CNQDs to check the importance of g-CNQDs in the binary MOF composite. g-CNQDs are well dispersed into the porous MOF surface which provides electronic stability to the binary MOF composite by minimizing the photogenerated electron-hole pair recombination rate, prolonging the fluorescence lifetime for photo induced carriers to enrich fluorescence emissions. The presence of electron-efficient surface charged groups (from g-CNQDs) and - NH_2 -BDC linker in the synthesized binary MOF composite enhances the fluorescence activity. The synthesized binary MOF composite (2), i.e., NH_2 -UiO-66/g-CNQDs (2), sensor exhibited quite excellent limit of detection (LOD) value of 2.4 nmol/L (~ 0.0006 mg/L) for mercury (II) in water which is even lesser than the permissible limit of mercury (II) in drinking water and the Stern-Volmer constant was found to be $K_{sv} \sim 2.3 \times 10^7$ L/mol. The detection capacity was found to be more effective for Hg^{2+} than some other interfering metal ions. To see the future applicability of the sensor towards real water sample analysis, we further tested this activity in some real water samples and have found good results. We ensured that the synthesized binary composite can be used as efficient sensor to detect Hg^{2+} in real water sample analysis.

1. Materials and methods

1.1. General characterization methods

All the chemicals and solvents (analytical reagent grade) were commercially available and used without further purification. The powder X-ray diffraction patterns (PXRDs) were recorded

on a Rigaku X-ray diffractometer (Ultima IV, Rigaku, Japan) equipped with Cu K α radiation. The Fourier transform infrared spectroscopy (FT-IR) data were measured by FTIR Spectrum-100 (Spectrum 100, PerkinElmer, USA) using KBr pellets. The specific surface area and porosities measurements were performed in Autosorb-iQ (Autosorb-iQ, Quantachrome, USA) analyzer using Brunauer-Emmett-Teller (BET) method. Thermogravimetric analysis (TGA) was performed on SDTQ600 analyzer (TA Instruments, USA) at a heating rate of 5°C/min under nitrogen atmosphere. Ultraviolet-visible (UV-Vis) spectra were performed on a SPECORD[®] 210 PLUS spectrophotometer (SPECORD[®] 210 PLUS, Analytik Jena, Germany) in the range 200–800 nm at room temperature. The sample morphologies were studied using high resolution transmission electron microscope (HRTEM) by JM-2100 Plus electron microscope (JEM2100 Plus, JEOL, USA) and field emission scanning electron microscope (FESEM) by Carl ZEISS scanning electron microscope (Σ IGMA, Carl ZEISS, Germany). The elemental compositions and energy dispersive X-ray (EDX) elemental mapping were obtained from energy dispersive X-ray spectroscopy (EDS) attached with FESEM. X-ray photoelectron spectroscopy (XPS) was recorded on ESCALAB Xi+ (EXCALAB Xi+, Thermo Fisher Scientific Pvt. Ltd., USA). Band gap energy were measured from UV-Vis diffuse reflectance spectra (DR-UV-Vis) using SPECORD[®] 210 PLUS spectrophotometer (SPECORD[®] 210 PLUS, Analytik Jena, Germany). The photoluminescence (PL) spectra and fluorescence lifetime were taken in Horiba Scientific Fluorolog-3 fluorescence spectrophotometer (FLUOROLOG-3, Horiba, Japan). The pH measurements were performed in μ pH system 362 (pH System 362, Systronics, India).

1.2. Synthesis of NH₂-UiO-66/g-CNQDs (2) binary composite

Similar synthetic methodology has been employed for synthesizing the binary MOF composite as reported earlier in our previous paper (Sonowal et al., 2022). ZrCl₄ (0.2332 g, 1 mmol) and 2-amino benzene dicarboxylic acid (NH₂-BDC ~ 0.1812 g, 1 mmol) were dissolved in 30 mL dimethylformamide (DMF) by ultrasonication. Then 3 mL of freshly prepared g-CNQDs solution was mixed well to the previous mixer of DMF solution. Then the whole solution was taken in a 100 mL Teflon-lined stainless-steel autoclave. The autoclave was sealed properly and heated at 130°C for 24 hr in an oven under autogenous pressure. After completion of the reaction, the autoclave was allowed to cool to room temperature. A gel form of product was obtained at first. Then the product was filtered with DMF several times then purified with acetone to make sure that the occluded DMF molecules were eliminated. Finally, a light yellowish powder was obtained which was dried under vacuum and the yield was found to be 0.405 g.

1.3. Complete materials synthesis

The detailed explanation of materials synthesis of NH₂-UiO-66 MOF, graphitic carbon nitride quantum dots and binary MOF composite series are given in part 1 of Appendix A Supplementary data.

1.4. General procedure for fluorescence measurements

The fluorescence measurements were taken using fluorescence spectrophotometer (FLUOROLOG-3, Horiba, Japan). Photoluminescence spectra (PL) for mercury (II) detection in water were performed adding 500 μ L neutral buffer and 30 μ L of 0.1 mg/mL MOF composite in a cuvette. Then 30 μ L of freshly prepared ten different concentrated mercury (II) solutions (0.001–0.019 μ mol/L) were added separately and the total volume of the solution was diluted to 3 mL with distilled water. The solution was mixed homogeneously, and fluorescence readings were taken at an excitation wavelength of 370 nm, fixing the slits at 5 nm. Similar procedure was repeated to study the mercury sensing activity by NH₂-UiO-66 and UiO-66 MOF. To confirm the highly selective nature of the sensor towards mercury (II) detection, fluorescence measurements were carried out with some other metal ions and anions (0.005 μ mol/L) in distilled water conducting the similar procedure. Time-resolved PL spectra were measured at room temperature using water as solvent for each material. Real water samples were analyzed with five different spiked mercury (II) concentrations using standard addition method (Table 1).

1.5. Real sample collection and pre-treatment

The real water samples include tap water, lake water and industrial water. The real water samples were collected and filtered using 0.25 μ m polyethersulfone (PES) membrane syringe filter (UNIFLO[®], Whatman[®], UK) to remove large impurities. The filtration process for each real water sample was repeated for two times and the fluorescence measurements of the sensor with spiked mercury concentrations were recorded taking the filtered real water sample. The photoluminescence spectra of the sensor in industrial water sample with spiked mercury concentrations were recorded after microfiltration and boiling. As the industrial wastewater may contain microorganisms which may absorb UV light and can produce background fluorescence at UV excitation during PL analysis. Therefore, pre-treatment like microfiltration and heating of such samples are essential before performing fluorescence measurements for detecting ions.

2. Results and discussion

The synthesized amino functionalized zirconium-based MOF incorporating g-CNQDs experiences loss in crystallinity and enhancement in the electronic properties after well dispersion of g-CNQDs as compared to that of parent NH₂-UiO-66 MOF due to highly electron efficient nature of g-CNQDs. The binary MOF composite exhibits excellent stability and acts as highly efficient luminescent sensor towards fluorescence sensing (Fig. 1) Fig. 1.

The as-synthesized binary MOF composite (NH₂-UiO-66/g-CNQDs) has been already reported in our previous work for photocatalytic CO₂ conversion into methanol (Sonowal et al., 2022). The code name for the binary MOF composite in our previous paper was reported as g-CNQDs@MOF. The same catalysts have been used here for studying the sensing activity

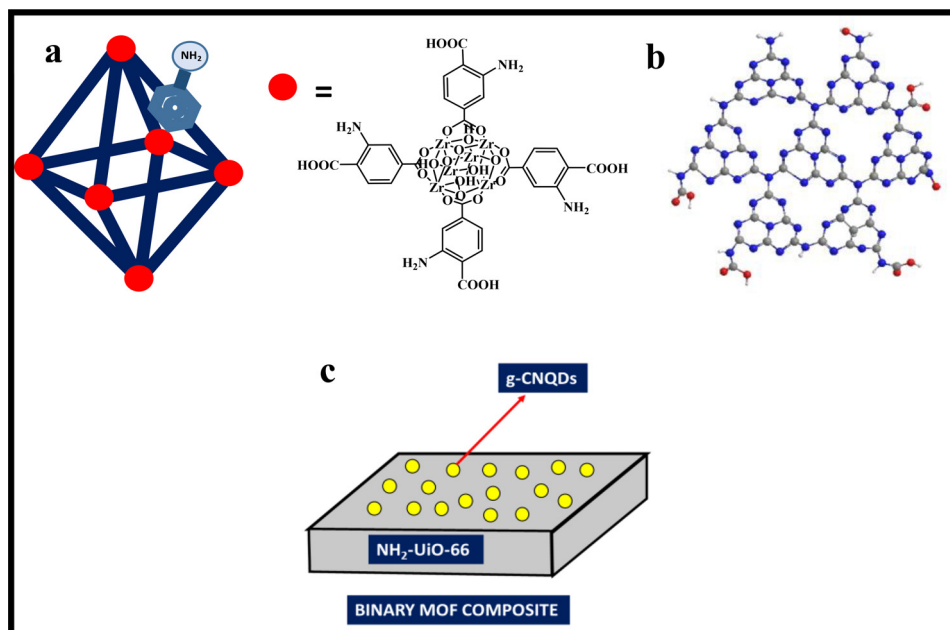


Fig. 1 – An overview of diagrammatic representation of (a) framework structure of NH₂-UiO-66, comprised of Zr₆O₄(OH)₄(CO₂)₁₂ octahedral secondary building unit (SBU) which has been represented by red colored symbol in (a), reported earlier by Kandiah et al., 2010a, (b) graphitic carbon nitride quantum dots (g-CNQDs) consisting of heptazine units as shown, reported earlier by Zhou et al., 2013a, and (c) a proposed view of as-synthesized NH₂-UiO-66/g-CNQDs binary metal-organic framework composite incorporating graphitic carbon nitride quantum dots on highly porous NH₂-UiO-66 MOF surface.

for mercury (II) in water. Therefore, the materials characterizations including PXRD, TGA, BET, XPS, UV-Vis, TEM and SEM analysis for NH₂-UiO-66/g-CNQDs, NH₂-UiO-66 and g-CNQDs have been referred to our previous paper where detail explanations were provided.

2.1. Characterization

Four binary MOF composites of NH₂-UiO-66/g-CNQDs at different stoichiometric proportions of ZrCl₄ (M) : 2-aminoterephthalic acid (L) : g-CNQDs were synthesized via *in situ* solvothermal synthetic technique, where M denotes metal and L denotes ligand. The composites were named as NH₂-UiO-66/g-CNQDs (1), NH₂-UiO-66/g-CNQDs (2), NH₂-UiO-66/g-CNQDs (3) and NH₂-UiO-66/g-CNQDs (4) synthesized at different stoichiometric ratio of M : L : g-CNQDs ~ 1 : 1 : 0.3, 1 : 1 : 1, 1 : 1 : 2, 1 : 1 : 3 respectively. Using the composites, fluorescence sensing study for mercury (II) detection in water was carried out by fluorescence spectrophotometer. Among the synthesized NH₂-UiO-66/g-CNQDs series, NH₂-UiO-66/g-CNQDs (2) exhibited highest fluorescence intensity and maximum fluorescent quenching in presence of 0.005 μmol/L mercury (II) ion as compared to that of the rest three MOF composites (Fig. 2). M : L : g-CNQDs (1 : 1 : 1) ratio can be considered as the optimal loading of g-CNQDs (3 mL, 0.002 mg/mL) on synthesizing the MOF composite in the given ratio for efficient fluorescence sensing of Hg²⁺ in water by the sensor. Therefore, highly fluorescent binary MOF composite (2) i.e., NH₂-UiO-66/g-CNQDs (2) with maximum quench-

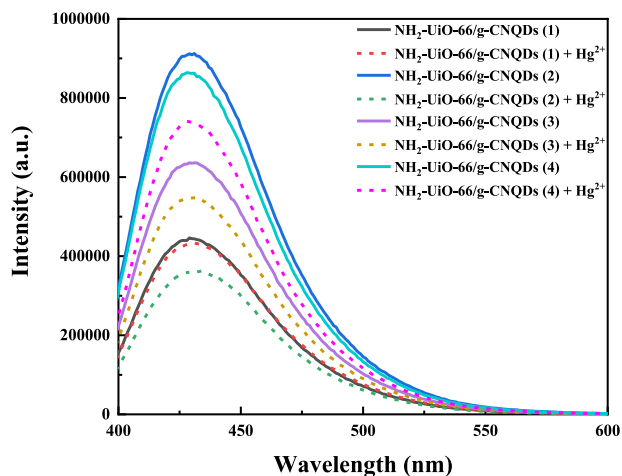


Fig. 2 – NH₂-UiO-66/g-CNQDs series showing highly fluorescent nature and maximum quenching for NH₂-UiO-66/g-CNQDs (2) composite (excitation at 370 nm) in presence of 0.005 μmol/L mercury (II) solution at similar composite concentration (0.1 mg/mL). Binary MOF composite (1) (NH₂-UiO-66/g-CNQDs (1)), binary MOF composite (2) (NH₂-UiO-66/g-CNQDs (2)), binary MOF composite (3) (NH₂-UiO-66/g-CNQDs (3)) and binary MOF composite (4) (NH₂-UiO-66/g-CNQDs (4)) synthesized at different stoichiometric ratio of metal : ligand : g-CNQDs ~ 1 : 1 : 0.3, 1 : 1 : 1, 1 : 1 : 2, and 1 : 1 : 3, respectively.

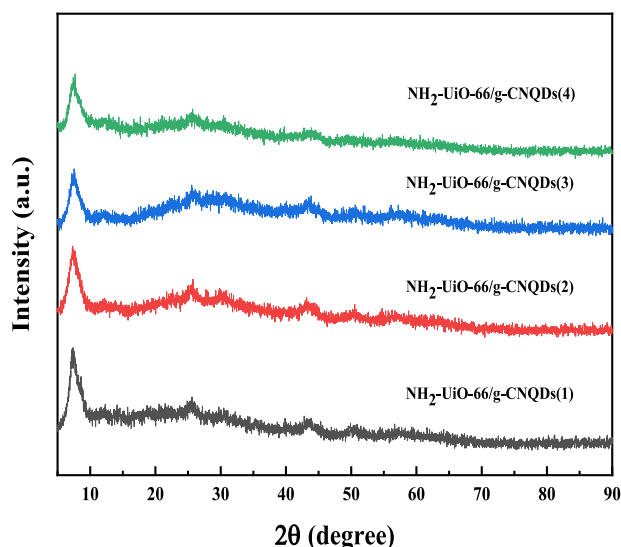


Fig. 3 – Powder X-ray diffraction patterns (PXRD) of NH₂-UiO-66/g-CNQDs at different stoichiometric proportions of added g-CNQDs.

ing activity with mercury (II) was considered for further analysis.

The phase purities of the binary MOF composites were studied by PXRD measurements as shown in Fig. 3. This was done to check the phase components purity and it was observed that on increasing the amount of added g-CNQDs, there is little decrease in the peak intensities gradually (from 1 to 4 as shown in Fig. 3). But 2θ positions remain unchanged and no new peak is observed. This is due to loading of quantum dots into MOF materials in small concentrations. Incorporation of g-CNQDs on Zr-based MOF enhanced the electronic properties but the crystallinity seemed to be lost as shown in Appendix A Fig. S1a. The enhancement in the electronic properties has been confirmed later from fluorescence measurement studies.

FT-IR analysis was performed for the synthesized materials, and it was found that the characteristic band of g-CNQDs at around 782 cm^{-1} is attributed to the heptazine unit which is the building block of g-CNQDs. The band at 1381 and 1413 cm^{-1} describes the CN heterocycle stretching vibrations and the band at 1630 and 3442 cm^{-1} depicts the carboxylate anion vibrational mode and O-H stretching mode of g-CNQDs, respectively. This confirms the presence of hydroxyl and carboxylate anions in g-CNQDs which matches the previous reports (Zhou et al., 2013). The FT-IR spectrum of the binary MOF composite (2) shows characteristic band positions at 3487 , 3347 , 2940 , 1655 , 1578 – 1336 , 1253 , 1107 , 772 – 662 cm^{-1} which is due to the presence of stretching modes of asymmetric amino stretching ($\nu(\text{NH}_2)_{\text{asym}}$), symmetric amino stretching ($\nu(\text{NH}_2)_{\text{sym}}$), C-H stretching ($\nu(\text{C-H})$), C=C stretching ($\nu(\text{C=C})$), aromatic stretching, CN stretching ($\nu(\text{CN})$), C-O stretching ($\nu(\text{C-O})$) and -C-H stretching ($\nu(-\text{C-H})$), respectively. The absorption peaks of the synthesized binary MOF composite (2) are found similar to that of parent NH₂-UiO-66 and no new generation of peaks of the binary MOF composite (2) is observed even af-

ter quantum dots incorporation. This is due to low content of g-CNQDs into porous MOF (Appendix A Fig. S1b).

To check the enhancement in the electronic properties of the binary MOF composite, fluorescence measurements were done. The binary MOF composite (2) and NH₂-UiO-66 MOF, both exhibit broad photoluminescence peak at 430 nm with intense blue color emissions as shown in Fig. 4a, signifying that electron-hole pairs can be sufficiently created and separated upon photon absorption in both the systems. The photoluminescence intensity of the binary MOF composite (2) increases as compared to that of parent NH₂-UiO-66 which is due to the presence of electron efficient g-CNQDs on MOF. The photoluminescent intensities of the synthesized MOF composites series were taken at similar composite concentrations (0.1 mg/mL) by fluorescence spectrophotometer (Fig. 4b) and was found that NH₂-UiO-66/g-CNQDs (2) acts as a highly fluorescent sensor as compared to the rest three MOF composites synthesized at different ratio. Therefore, it was considered for further experiment. Though fluorescence intensity increases with increasing amount g-CNQDs, after a certain limit the fluorescence intensity seemed to be decreased as can be observed in case of MOF composite (3) and (4). This may be due to the accumulation of excess g-CNQDs on porous MOF surface that blocks the pores of NH₂-UiO-66 MOF sufficiently and reduces the activity of functional amino group present in the binary MOF composite. As the amino group connected to the benzene dicarboxylate linker in MOF is one the main reasons for enhancing the luminescence property of NH₂-UiO-66 MOF.

Incorporation of g-CNQDs into MOF decreased the band gap energy of the binary MOF composite from 2.70 to 2.57 eV which were confirmed from Tauc plots as shown in Appendix A Fig. S2a. The time resolved PL spectra gives the fluorescence lifetime of the synthesized materials. The average lifetime of NH₂-UiO-66, g-CNQDs and NH₂-UiO-66/g-CNQDs (2) are found to be 0.71 , 7.95 and 13.43 nsec respectively (Appendix A Fig. S2b). There is a huge increase in average lifetime after incorporation of g-CNQDs into the porous framework which confirms that incorporation of g-CNQDs into metal-organic framework minimizes the electron-hole pair recombination rate of the composite and prolongs the lifetime of photogenerated electron-hole pairs. This demonstrates that the synthesized binary composite (2) can act as an efficient sensor for fluorescence sensing applications further providing electronic stability to the sensor.

The Mott-Schottky analysis of NH₂-UiO-66/g-CNQDs was performed to know the band energies (Fig. 5). The flat band potential (V_{fb}) for the binary MOF composite was found to be -0.46 V and the negative flat band potential of the binary MOF composite signifies the n-type semiconducting nature. It has been found from literature that n-type semiconductors have conduction band energy highly negative by 0.15 V as compared to V_{fb} (Jiang et al., 2017; Zhang et al., 2018). Therefore, the conduction band (CB) or lowest unoccupied molecular orbital (LUMO) and the valence band (VB) or highest occupied molecular orbital (HOMO) energies for the binary MOF composite were measured to be -0.31 and 2.26 V , respectively. Mott-Schottky analysis was performed in 0.1 mol/L aqueous KHCO_3 solution at 100 Hz frequency using Ag/AgCl as reference electrode.

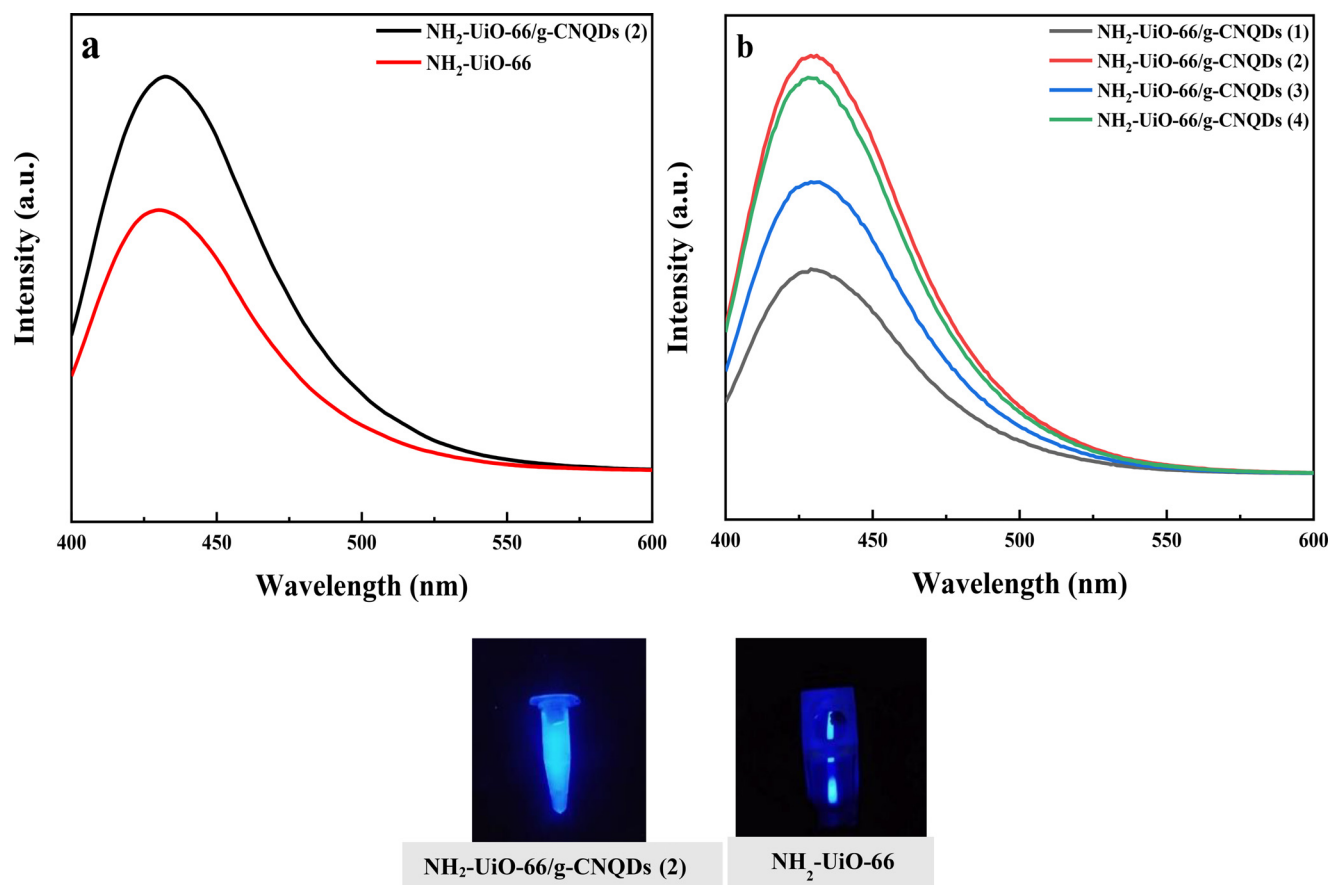


Fig. 4 – (a) Photoluminescence spectra of as-synthesized $\text{NH}_2\text{-UiO-66}$ MOF and $\text{NH}_2\text{-UiO-66/g-CNQDs (2)}$ at an excitation of 370 nm and (b) photoluminescence spectra for binary MOF composites series at same composite concentration.

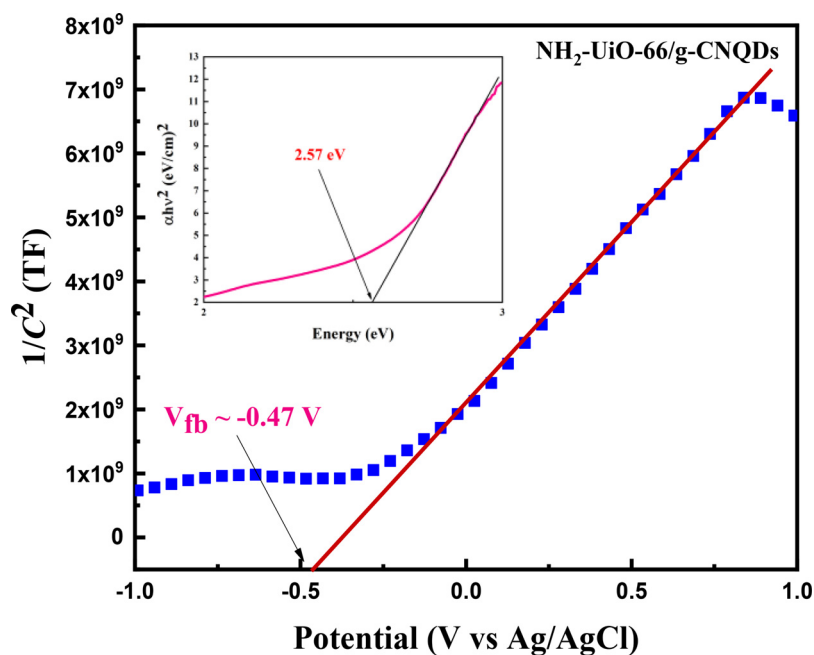


Fig. 5 – Mott-Schottky plot of $\text{NH}_2\text{-UiO-66/g-CNQDs (2)}$. Inset: Tauc plot representing band gap of $\text{NH}_2\text{-UiO-66/g-CNQDs (2)}$. TF: terafarad; V_{fb} : flat band potential; α : absorption coefficient; $h\nu$: photon energy.

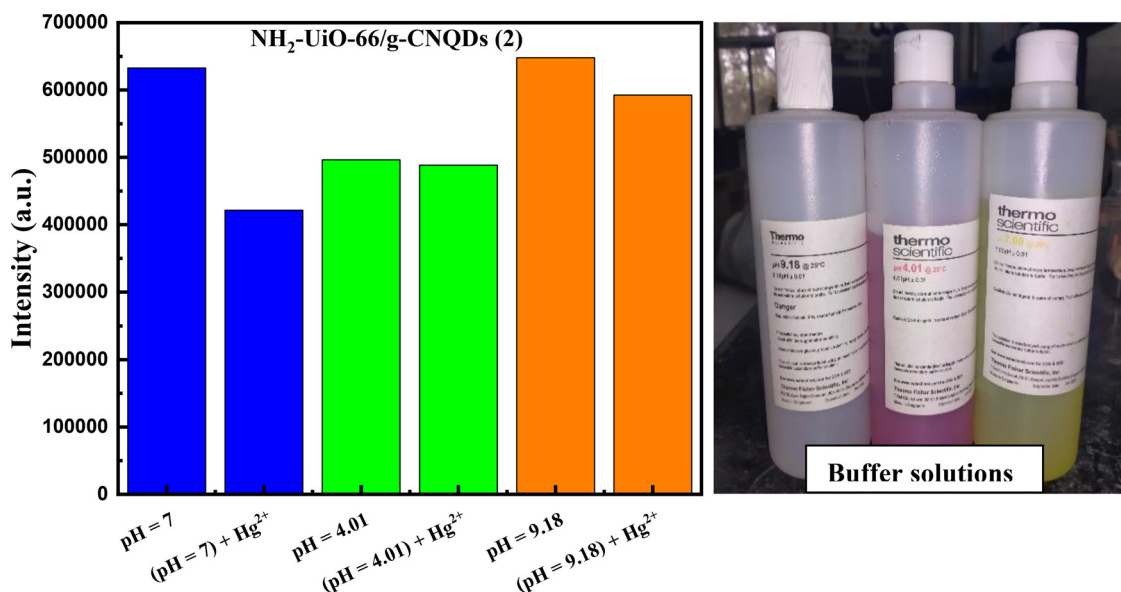


Fig. 6 – Fluorescence measurements of the binary MOF composite (2) with and without addition of mercury (II) at different pH medium.

2.2. pH effect study on fluorescence sensing towards Hg²⁺ detection

To study the pH effect of the binary MOF composite towards sensing activity, three different buffer solutions (acidic, basic and neutral) were used to maintain the perfect pH. The binary MOF composite (2) exhibited highest sensitivity towards mercury (II) detection at neutral pH (pH = 7) as compared to acidic (pH = 4.01) and basic (pH = 9.18) conditions. The binary composite at pH = 7 exhibited maximum fluorescent quenching in presence of mercury (II) than acidic and basic pH. The highest quenching at neutral condition may be attributed to the balanced charge transfer interactions between the sensor and the quencher. At acidic pH, due to the generation of more acidic protons on the surface of binary MOF composite (2), the PL intensity was seemed to be decreased and the observed fluorescence quenching was seemed to be the least in presence of mercury (II) than neutral and basic medium. At basic pH, a little increase in PL intensity of binary MOF composite (2) as compared to neutral pH was observed which could be due to increase of basic hydroxyl groups on the surface of binary MOF composite (2) but the quenching was less. Since, the binary MOF composite (2) exhibited highest fluorescence quenching at neutral pH. Therefore, the binary MOF composite (2) at neutral pH was considered for studying the sensing activity towards mercury (II) detection in water.

2.3. Detection of Hg²⁺ ion in water based on fluorescence quenching method (pH = 7)

The photoluminescent properties were studied for the synthesized binary composite at room temperature condition. The binary MOF composite (2) showed a quantum yield of 71%. To check the fluorescence sensing activity of the sensor towards mercury (II), 1000 μmol/L stock solution of mercury (II) in 10 mL distilled water was prepared at first and

by dilution method, ten different concentrated solutions of mercury (II) like 0.001, 0.003, 0.005, 0.007, 0.009, 0.011, 0.013, 0.015, 0.017, 0.019 μmol/L were prepared. There was no color change of the binary MOF composite solution after addition of mercury (II) solution and fluorescence measurement readings were taken. It was found that with increase in the concentrations of spiked Hg²⁺, the fluorescence intensities of the binary MOF composite (2) decrease gradually (Fig. 7a). Mercury (II) addition to the binary MOF composite (2) results in turn-off fluorescence quenching of PL intensities of the synthesized binary MOF composite (2). The quenching effect can be studied by Stern-Volmer equation:

$$F_0/F = 1 + K_{SV}[Q] \tag{1}$$

where, F₀ and F represents fluorescent intensity of the suspension at a particular wavelength in the absence and presence of quencher respectively, K_{SV} (L/mol) is the Stern-Volmer constant and [Q] (μmol/L) is the concentration of the quencher. In this work, [Q] = [Hg²⁺] and NH₂-UiO-66/g-CNQDs (2) sensor exhibited linear response towards Hg²⁺ with LOD value of 2.4 nmol/L. The LOD value was calculated using the following formula:

$$LOD = 3S_b/S \tag{2}$$

where

$$S_b = \sqrt{\frac{\sum (F - F_0)^2}{(X - 1)}} \tag{3}$$

where, signal / noise = 3, S is the slope of Stern-Volmer linear relationship, S_b is the standard deviation, X represents total number of readings taken (X = 10), F₀ is the intensity of blank solution and F is the average intensity after addition of quencher. From the calibration curve, we can get the values of slope (S) and standard deviation (S_b) can be calculated, that would lead to find out LOD value which is a very important factor for the luminescent quenching method. Fig. 7b is the

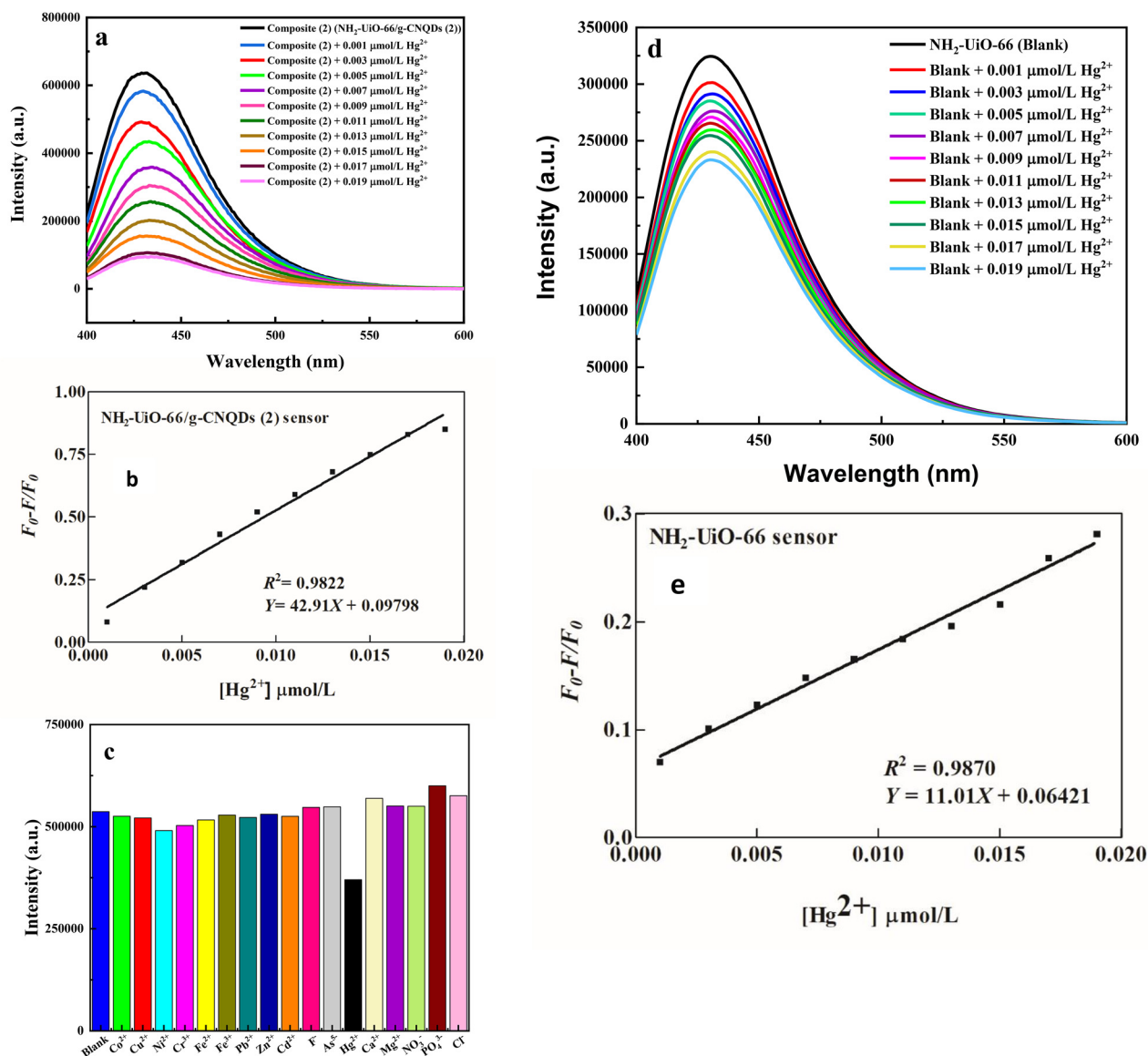


Fig. 7 – (a) Fluorescence sensing by $\text{NH}_2\text{-UiO-66/g-CNQDs (2)}$ dispersed in water with spiked HgCl_2 concentrations at an excitation of 370 nm, (b) Stern-Volmer plot of $\text{NH}_2\text{-UiO-66/g-CNQDs (2)}$ sensor for limit of detection (LOD) calculation with good linearity, $R^2 = 0.9822$, (c) fluorescence response of $\text{NH}_2\text{-UiO-66/g-CNQDs (2)}$ with different interfering metal ions and anions in water, (d) fluorescence sensing using $\text{NH}_2\text{-UiO-66}$ dispersed in water with gradual addition of Hg^{2+} , at an excitation of 370 nm and (e) Stern-Volmer plot of $\text{NH}_2\text{-UiO-66}$ sensor for LOD measurement with good linearity, $R^2 = 0.9870$. F_0 : fluorescence intensity of the blank; F : fluorescence intensity after quencher addition.

Stern-Volmer plot showing the linear relationship of mercury (II) concentration with the quenching efficiency ($F_0 - F/F_0$). The Stern-Volmer constant (K_{sv}) was found to be $\sim 2.3 \times 10^7$ L/mol.

To prove the highly selective nature of the sensor towards mercury (II) sensing, the fluorescence spectrophotometry analysis of the sensor was carried out with some other interfering metal ions such as Co^{2+} , Cu^{2+} , Ni^{2+} , Cr^{3+} , Fe^{2+} , Fe^{3+} , Pb^{2+} , Zn^{2+} , Cd^{2+} , F^- , As^{5-} , Ca^{2+} , Mg^{2+} , NO_3^- , PO_4^{3-} , Cl^- at room temperature. It was monitored that the sensor shows high selectivity towards mercury (II) detection in water than the other metal ions and anions as shown in Fig. 7c. It elucidates that Hg^{2+} exhibits significant turn-off fluorescent quenching rather than the other ions in water.

To see the effectiveness of the sensor $\text{NH}_2\text{-UiO-66/g-CNQDs (2)}$ towards mercury (II) detection in water, a comparative study with $\text{NH}_2\text{-UiO-66}$ MOF was carried out which proves the importance and efficiency of g-CNQDs in the binary MOF composite (2). For this, the sensing activity of $\text{NH}_2\text{-UiO-66}$ MOF towards mercury (II) detection in water was carried out in the similar range (0.001–0.019 $\mu\text{mol/L}$) and the limit of detection was found to be 6.5 nmol/L (0.0016 mg/L) (Fig. 7d). It was observed that the LOD value for $\text{NH}_2\text{-UiO-66}$ sensor is higher as compared to the binary MOF composite (2), proving that the presence of g-CNQDs in the binary MOF composite (2) enhances the mercury (II) detection capacity in water which results in excellent LOD value of binary MOF compos-

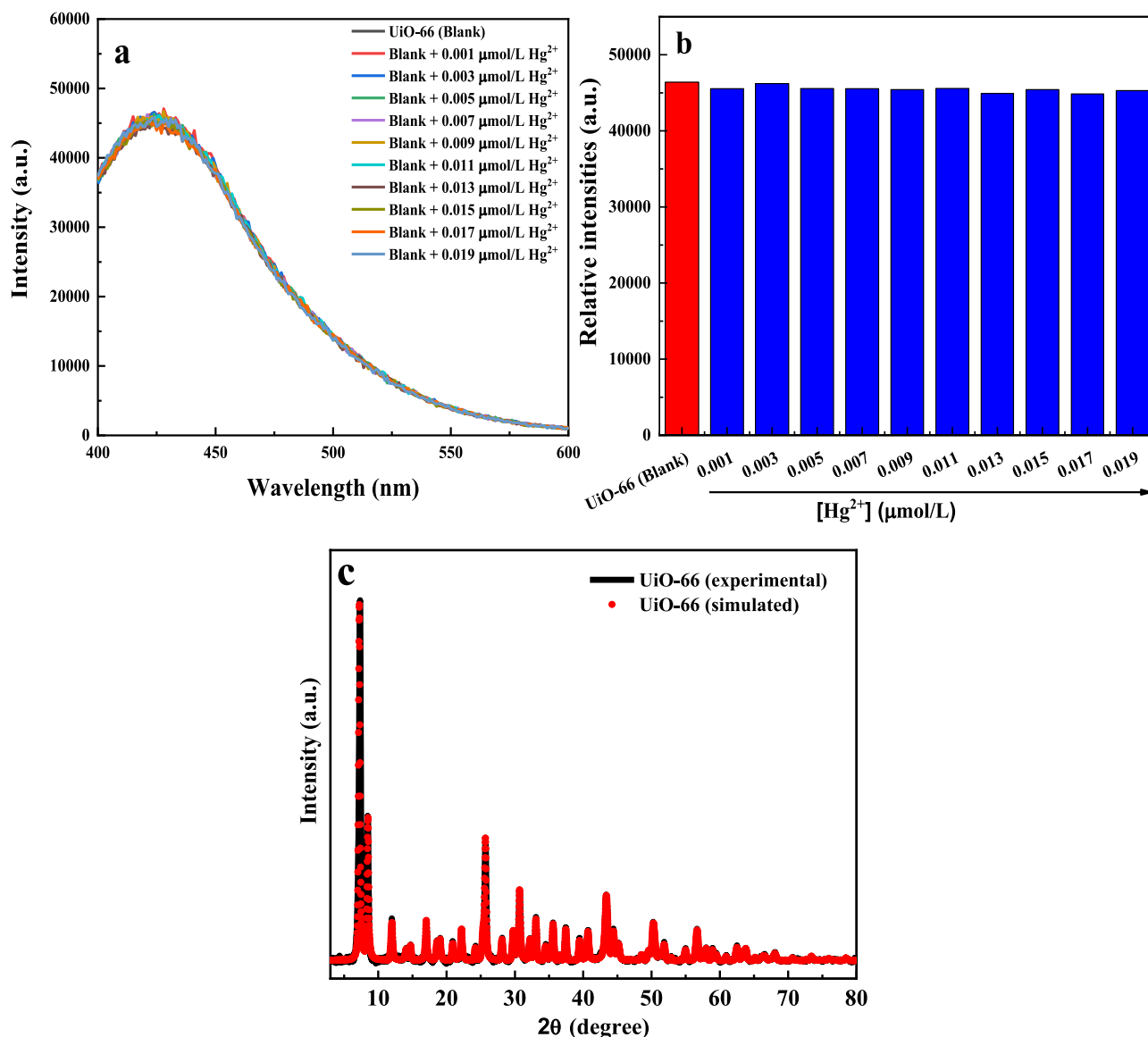


Fig. 8 – (a) Fluorescence sensing by UiO-66 MOF dispersed in water with gradual addition of Hg²⁺, at an excitation of 370 nm, (b) bar diagram representation of (a), and (c) powder X-ray diffraction pattern of experimental UiO-66 MOF with simulated X-ray diffraction pattern.

ite (2) as compared to that of parent NH₂-UiO-66 sensor. The Stern-Volmer plot for NH₂-UiO-66 MOF is plotted as quenching efficiency ($F_0 - F/F_0$) vs mercury (II) concentration as shown in Fig. 7e.

In order to check the importance of -NH₂ group in the UiO-66 MOF, fluorescence sensing was performed with UiO-66 MOF at similar range of spiked mercury (II) concentration (0.001–0.019 μmol/L) and it was found that UiO-66 MOF is not capable to detect mercury (II) in water in the range of 0.001–0.019 μmol/L (Fig. 8a and b). Therefore, no change in fluorescence intensity of UiO-66 was detected by fluorescence spectrometry analysis. It proves that presence of amino group has vital role in the binary MOF composite for high light absorption capability and electron donating capacity. UiO-66 cannot act as a sensor for mercury (II) detection in water in the

spiked mercury (II) concentrations. UiO-66 MOF was synthesized successfully via solvothermal synthesis technique from a DMF solution containing ZrCl₄ and terephthalic acid, heated at 130°C for 24 hr using similar procedure reported earlier by Kandiah et al. (2010a) only changing temperature parameter. To confirm the formation of UiO-66 metal-organic framework, PXRD measurement of as-synthesized UiO-66 MOF with simulated XRD patterns (Joint Committee Powder Diffraction Standards (JCPDS) No. 01-085-6809) is provided (Fig. 8c).

The NH₂-UiO-66/g-CNQDs (2) sensor exhibited good water stability and strong fluorescence emissions in water. The water stability has been confirmed by PXRD measurement. No change in the 2θ positions of PXRD patterns was observed even after immersion of the sensor in water for one week (Appendix A Fig. S3a) which confirms that the sensor is stable in

water. The fluorescence stability of NH₂-UiO-66/g-CNQDs (2) and NH₂-UiO-66 sensor were studied and found that both exhibit good fluorescence stability which can be confirmed by fluorescence measurements (Appendix A Fig. S3b).

As mentioned above, many sensors are not stable in water, for those organic solvents like ethanol, methanol, dimethylformamide, dimethyl sulfoxide (DMSO) etc. solvents are used to carry out sensing applications which are cost effective and thus limit their applications to some point somehow. Lots of work on fluorescent sensing using lanthanide-based MOFs as sensors are going on using water as medium with good results, but most of these lanthanide-based MOF sensors based on cation exchange process (Cao et al., 2015; Wang et al., 2014; Zhou et al., 2014). This cation exchange limits the utilization of such sensors due to time consuming, less efficiency and post-treatment of sensor. Still, variety of fluorescence sensing systems including MOF based sensors have been reported so far for the detection of heavy metal ions in water. That is why, it is becoming more challenging nowadays to design efficient fluorescent sensors for sensing heavy metal ions in water with better selectivity and sensitivity. From all these, it can be confirmed that NH₂-UiO-66/g-CNQDs (2) is one of the most promising sensors with good water and fluorescence stability to be used in the fluorescence sensing of Hg²⁺ in water with good selectivity and sensitivity.

2.4. Real water sample analysis

Further, to check the future applicability of the sensor towards real water sample analysis, we tested the fluorescence sensing with some real water samples by standard addition method. Five different concentrated solutions 0.011, 0.013, 0.015, 0.017, 0.019 μmol/L of Hg²⁺ in each type of water samples were taken and the fluorescence measurements were recorded using fluorescence spectrophotometer. It was found that the detected Hg²⁺ amounts by the sensor were almost similar with the spiked amounts of Hg²⁺ as shown in Table 1. This signifies that the NH₂-UiO-66/g-CNQDs (2) sensor can be used effec-

tively for the detection of Hg²⁺ in real water samples using this method.

The results are executed as mean value of five measurements ± standard deviation (SD) and percentage recovery has been calculated as (found Hg²⁺ / spiked Hg²⁺) × 100%.

2.5. Fluorescence quenching mechanism

The sensing mechanism was studied for NH₂-UiO-66/g-CNQDs (2) sensor. From PXRD measurements of the sensor after mercury (II) addition, it is observed that there is no change in the 2θ positions of the PXRD patterns (Appendix A Fig. S4a) which indicates that no new phases are generated because of mercury (II) ions of the sensor, i.e., mercury (II) interaction. Mercury (II) does not show any bonding interaction with the sensor, instead it easily gets diffused into the channels of the framework structure for which it exhibits quick response towards fluorescence sensing. Also, presence of no bonding interaction between the sensor and Hg²⁺ ions is also confirmed from FT-IR measurements as shown in Appendix A Fig. S4b.

From the above results of our work, it is presumed that only charge transfer interactions can be present between the sensor and the quencher. For fluorescence sensing, there are three different types of quenching that can happen which were found from literature (Dong et al., 2015; Wang et al., 2018a; Xiang et al., 2014). These are (i) dynamic quenching, (ii) static quenching, and (iii) inner-filter quenching (IFQ).

In this work, the fluorescence lifetime of the sensor, NH₂-UiO-66/g-CNQDs (2) after mercury (II) (quencher (Q)) addition was found to be decreased than without mercury (II) addition which represents dynamic fluorescence quenching (Appendix A Fig. S5). The calculated fluorescence lifetime of the sensor reduced after addition of Hg²⁺ ion solutions from 25.75 to 5.44 nsec. The possible electron transfer process between the sensor and the quencher was further studied and was found that photoinduced electron transfer (PET) process was responsible for fluorescence quenching as shown in Fig. 9. The interaction between the luminescent substances present in the sensor (host) and the incoming guest species (such as

Table 1 – Mercury (II) determination by NH₂-UiO-66/g-CNQDs (2) sensor in real water samples using standard addition method.

Water type	Spiked Hg ²⁺ concentration (μmol/L)	Found Hg ²⁺ concentration (μmol/L)	Recovery
Tap water	0.011	0.010 ± 0.004	90.9%
	0.013	0.012 ± 0.002	92.3%
	0.015	0.015 ± 0.001	100%
	0.017	0.016 ± 0.002	94.11%
	0.019	0.018 ± 0.003	94.73%
Lake water	0.011	0.010 ± 0.002	90.9%
	0.013	0.013 ± 0.002	100%
	0.015	0.015 ± 0.001	100%
	0.017	0.016 ± 0.002	94.11%
	0.019	0.016 ± 0.003	84.21%
Industrial water	0.011	0.011 ± 0.001	100%
	0.013	0.012 ± 0.002	92.3%
	0.015	0.015 ± 0.001	100%
	0.017	0.016 ± 0.003	94.11%
	0.019	0.019 ± 0.001	100%

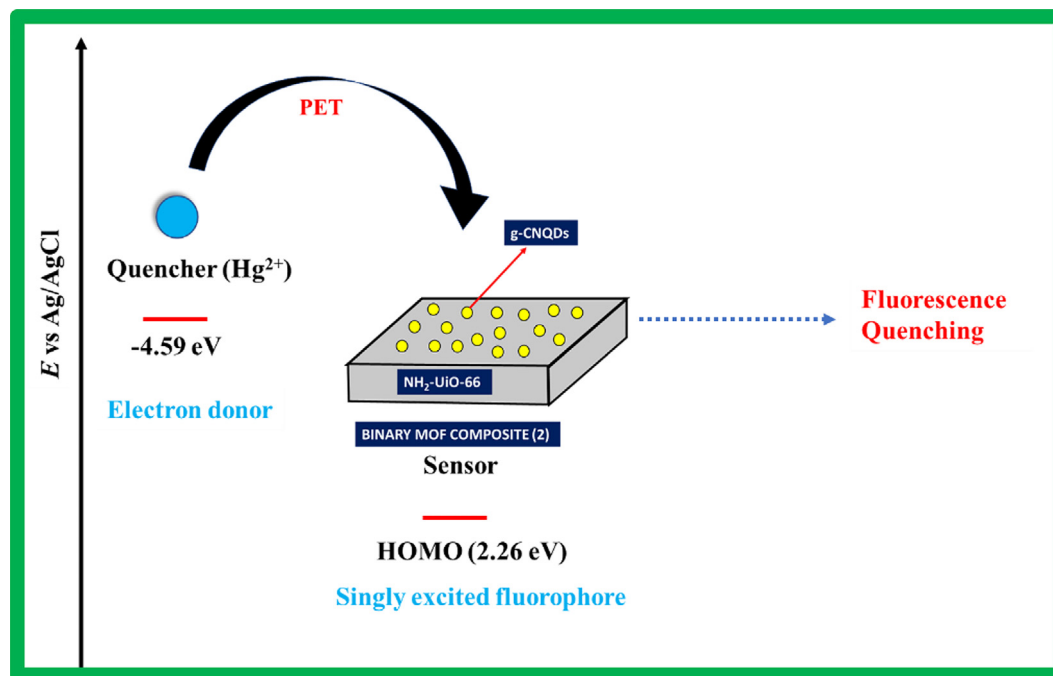


Fig. 9 – Proposed fluorescence quenching mechanism, representing highest occupied molecular orbital (HOMO) of the sensor and the highest occupied orbital of mercury (II) responsible for photoinduced electron transfer (PET) process. E: potential in electron volt.

metal ions or quencher) brings about the energy transfer processes (Aigner et al., 2011; Briggs and Besley, 2015; David, 2015; Fan et al., 2009; Formica et al., 2012; Nagarkar et al., 2013; Pramanik et al., 2011; Wang et al., 2017a, 2016). PET is a process of energy transfer where energy in the form of electrons gets transferred from one fluorophore (donor) to another fluorophore (acceptor) via redox non-radiative pathway. The redox reactions are created by the delocalized electrons present in the conjugated system provided by the ligands in the fluorophore. In this work, the presence of highly conjugated system with enriched functional groups like hydroxyl, carboxylate and amino groups contributes large number of delocalized electrons to the fluorophore sensor. Additionally, the quencher (Hg^{2+}) has highly filled d-orbitals (d^{10}) in it. The HOMO of the sensor is mostly contributed by the electron-efficient ligands and the LUMO by vacant d-orbital of Zr^{4+} center. In presence of light, the delocalized electrons from the ground state of the sensor (HOMO) gets excited into the excited state (LUMO) providing singly excited fluorophore sensor. Due to instability of the excited electrons, the electrons fall back into the ground state yielding fluorescence. While in contact with the quencher (Hg^{2+} here acts as donor fluorophore with highly filled d-orbitals), the electrons from the highest occupied orbital of mercury (II) gets transferred to the HOMO of the singly excited sensor following up a redox non-radiative pathway. As a result, the fluorescence emissions of the sensor are quenched. Since the vacant positive space in HOMO of the singly excited fluorophore sensor will be occupied by single electron from quencher Hg^{2+} . Therefore, the already excited electron of the sensor can't fall back to the ground state to yield fluorescence. This process of electron

transfer between the sensor and the quencher is known as PET process.

The synergistic effect of $\text{NH}_2\text{-Uio-66}$ MOF and g-CNQDs is the main cause for the enhancement of fluorescence quenching activity after mercury (II) addition than the sole MOF. Presence of g-CNQDs in MOF enhances the fluorescence quenching in presence of mercury (II) which may be attributed to the mercury (II) interaction with electron efficient N atom of conjugated heptazine unit or -OH groups of g-CNQDs that may bring g-CNQDs close to each other (Wang et al., 2018c). This further confirms the possible PET interaction between the sensor and the quencher which results in reduced fluorescence intensity.

To evaluate the potential values of Hg^{2+} , cyclic voltammetry (CV) analysis of mercuric chloride was carried out in 0.1 mol/L Na_2SO_4 aqueous solution using Ag/AgCl as reference electrode and at 1 mA current. The oxidation potential (E_{oxd}) for mercury (II) formation was found to be 0.223 V vs Ag/AgCl (Fig. 10). From literature, it is found that orbital energies can also be calculated from CV analysis considering standard potential values for ferrocene (Fc). The standard potential values considered for ferrocene from literature were obtained as, $E_{\text{HOMO}}[\text{Fc}] = -4.78$ eV and $E_{0.5}^{\text{oxd}}[\text{Fc}] = +0.405$ eV (Thorat et al., 2015) where $E_{\text{HOMO}}[\text{Fc}]$ signifies energy of highest occupied molecular orbital of ferrocene and $E_{0.5}^{\text{oxd}}[\text{Fc}]$ signifies potential of oxidation half reaction of ferrocene. The energy of highest occupied orbital of mercury (II) ($E_{\text{HOMO}}[\text{Hg}^{2+}]$) was calculated to be -4.59 eV. The formula used to calculate the HOMO energy of mercury (II) ion is as follows:

$$E_{\text{HOMO}}[\text{Hg}^{2+}] = E_{\text{HOMO}}[\text{Fc}] + (E_{0.5}^{\text{oxd}}[\text{Fc}] - E_{0.5}^{\text{oxd}}[\text{Hg}^{2+}]) \quad (4)$$

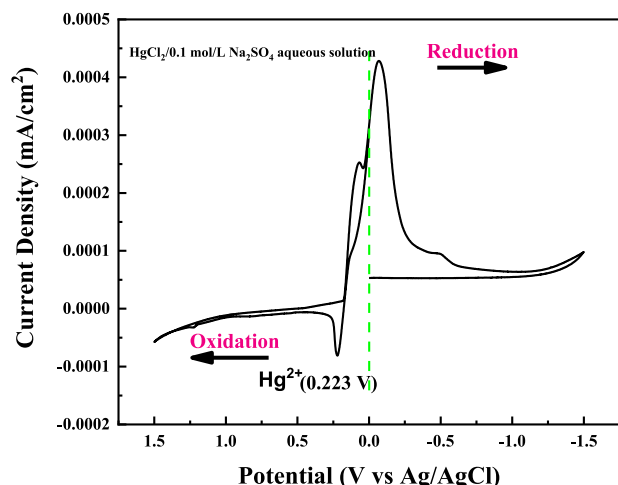


Fig. 10 – Cyclic voltammogram for mercury (II) in 0.1 mol/L Na_2SO_4 aqueous solution using Ag/AgCl as reference electrode.

3. Conclusions

Briefly, it can be concluded that highly fluorescent binary MOF composite (2) has been synthesized successfully via *in-situ* solvothermal technique. The incorporation of graphitic carbon nitride quantum dots into MOF explores the highly fluorescent nature of this semiconducting material with excellent electronic stability. This leads to see its applicability towards fluorescence sensing for detection of metal ions like mercury (II) in water and it has been found that $\text{NH}_2\text{-UiO-66/g-CNQDs}$ (2) acts as a highly efficient fluorescent sensor for sensing Hg^{2+} selectively in water. The sensor exhibited distinct fluorescence quenching in presence of Hg^{2+} with an excellent limit of detection of 2.4 nmol/L (0.0006 mg/L). The LOD value was found to be excellent than the permissible limit of mercury (II) in drinking water and some previous reports for mercury (II) detection. According to World Health Organization (WHO) and Indian Standard Bureau (ISB), the permissible limit of mercury (II) in drinking water is 0.001 mg/L. Further, the sensor was used to see its applicability towards real water sample analysis and was found effective results with excellent detection capacity and good recovery rate. The sensor exhibits dynamic fluorescence quenching and PET electron transfer process in presence of quencher. The presence of electron-efficient ligands and functional groups in the sensor molecule stimulates the fluorescence sensing activity overall for metal ions detection in water providing electronic stability to the sensor, also prolonging the fluorescence lifetime of the photo-induced charge carriers. The synergistic effect between MOF and g-CNQDs enhanced mercury detection capacity than sole MOF. Thus, the sensor can be used as a highly sensitive and selective probe to probe Hg^{2+} in water even in presence of other interfering metal ions with good precisions and good water stability.

Acknowledgments

The authors are thankful to the Director, Council of Scientific and Industrial Research (CSIR)-North East Institute of Science and Technology, Jorhat, Assam, India, for his kind support and allowance to publish the research work. Karanika Sonowal and Lakshi Saikia acknowledge University Grants Commission (UGC)-New Delhi for CSIR-UGC (NET) fellowship and In-house project for financial support.

Appendix A Supplementary data

Supplementary material associated with this article can be found in the online version at doi:10.1016/j.jes.2022.05.032.

REFERENCES

- Aguilera-Sigalat, J., Bradshaw, D., 2016. Synthesis and applications of metal-organic framework-quantum dot (QD@MOF) composites. *Coord. Chem. Rev.* 307, 267–291.
- Aigner, D., Borisov, S.M., Klimant, I., 2011. New fluorescent perylene bisimide indicators - a platform for broadband pH optodes. *Anal. Bioanal. Chem.* 400, 2475–2485.
- Briggs, E.A., Besley, N.A., 2015. Density functional theory-based analysis of photoinduced electron transfer in a triazacrypt and based K^+ sensor. *J. Phys. Chem. A* 119, 2902–2907.
- Cao, L.-H., Shi, F., Zhang, W.-M., Zang, S.-Q., Mak, T.C.W., 2015. Selective sensing of Fe^{3+} and Al^{3+} ions and detection of 2,4,6-trinitrophenol by a water-stable terbium-based metal-organic framework. *Chem. Eur. J.* 21 (44), 15705–15712.
- Chen, G.H., He, Y.P., Zhang, S.H., Zhang, J., 2019. Syntheses, crystal structures and fluorescent properties of two metal-organic frameworks based on pamoic acid. *J. Solid State Chem.* 270, 335–338.
- Chen, S., Feng, F., Li, S., Li, X.X., Shu, L., 2018. Metal-organic framework dut-67(Zr) for adsorptive removal of trace Hg^{2+} and CH_3Hg^+ in water. *Chem. Speciat. Bioavailab.* 30, 99–106.
- David, C.M., 2015. Photoinduced electron transfer as a design concept for luminescent redox indicators. *Analyst* 140, 7487–7495.
- Deng, Y., Chen, Y., Zhou, X., 2018. Simultaneous sensitive detection of lead (II), mercury (II) and silver ions using a new nucleic acid-based fluorescence sensor. *Acta Chim. Slov.* 65, 271–277.
- Dong, X.-Y., Wang, R., Wang, J.-Z., Zang, S.-Q., Mak, T.C.W., 2015. Highly selective Fe^{3+} sensing and proton conduction in a water-stable sulfonate-carboxylate Tb-organic-framework. *J. Mater. Chem. A* 3, 641–647.
- Fan, L.J., Zhang, Y., Murphy, C.B., Angell, S.E., Parker, M.F.L., Flynn, B.R., et al., 2009. Fluorescent conjugated polymer molecular wire chemosensors for transition metal ion recognition and signaling. *Coord. Chem. Rev.* 253, 410–422.
- Fang, X., Zong, B., Mao, S., 2018. Metal-organic framework-based sensors for environmental contaminant sensing. *Micro Nano Lett.* 10, 64.
- Formica, M., Fusi, V., Giorgi, L., Micheloni, M., 2012. New fluorescent chemosensors for metal ions in solution. *Coord. Chem. Rev.* 256, 170–192.
- Gustafsson, M., Bartoszewicz, A., Martín-Matute, B., Sun, J., Grins, J., Zhao, T., et al., 2010. A family of highly stable lanthanide metal-organic frameworks: Structural evolution and catalytic activity. *Chem. Mater.* 22, 3316–3322.

- Jiang, D., Wang, T., Xu, Q., Li, D., Meng, S., Chen, M., 2017. Perovskite oxide ultrathin nanosheets/g-C₃N₄ 2D-2D heterojunction photocatalysts with significantly enhanced photocatalytic activity towards the photodegradation of tetracycline. *Appl. Catal. B* 201, 617–628.
- Jin, M., Mou, Z.L., Zhang, R.L., Liang, S.S., Zhang, Z.Q., 2017. An efficient ratiometric fluorescence sensor based on metal-organic frameworks and quantum dots for highly selective detection of 6-mercaptopurine. *Biosens. Bioelectron.* 91, 162–168.
- Kandiah, M., Nilsen, M.H., Usseglio, S., Jakobsen, S., Olsbye, U., Tilset, M., et al., 2010a. Synthesis and stability of tagged UiO-66 Zr-MOFs. *Chem. Mater.* 22, 6632–6640.
- Kandiah, M., Usseglio, S., Svelle, S., Olsbye, U., Lillerud, K.P., Tilset, M., 2010b. Post-synthetic modification of the metal-organic framework compound UiO-66. *J. Mater. Chem.* 20, 9848–9851.
- Li, Y.-F., Wang, D., Liao, Z., Kang, Y., Ding, W.-H., Zheng, X.-J., et al., 2016. Luminescence tuning of the Dy-Zn metal-organic framework and its application in the detection of Fe(III) ions. *J. Mater. Chem. C* 4, 4211–4217.
- Li, Y.-J., Wang, Y.-L., Liu, Q.-Y., 2017. The highly connected MOFs constructed from nonanuclear and trinuclear lanthanide-carboxylate clusters: selective gas adsorption and luminescent pH sensing. *Inorg. Chem.* 56, 2159–2164.
- Liu, J., Vellaisamy, K., Yang, G., Leung, C.-H., Ma, D.-L., 2017. Luminescent turn-on detection of Hg(II) via the quenching of an iridium (III) complex by Hg(II)-mediated silver nanoparticles. *Sci. Rep.* 7 (1), 3620.
- Liu, J., Yang, G.P., Jin, J., Wu, D., Ma, L.F., Wang, Y.Y., 2020. A first new porous d-p HMOF material with multiple active sites for excellent CO₂ capture and catalysis. *Chem. Commun.* 56, 2395–2398.
- Luo, T., Zhang, J., Li, W., He, Z., Sun, X., Shi, J., et al., 2017. Metal-organic framework-stabilized CO₂/water interfacial route for photocatalytic CO₂ conversion. *ACS Appl. Mater. Interfaces* 9, 41594–41598.
- Ma, S., 2009. Gas adsorption applications of porous metal-organic frameworks. *Pure Appl. Chem.* 81, 2235–2251.
- Mirnajafzadeh, F., Ramsey, D., McAlpine, S., Wang, F., Stride, J.A., 2019. Nanoparticles for bioapplications: Study of the cytotoxicity of water dispersible CdSe(S) and CdSe(S)/ZnO quantum dots. *Nanomaterials* 9 (3), 465.
- Nagarkar, S.S., Joarder, B., Chaudhari, A.K., Mukherjee, S., Ghosh, S.K., 2013. Highly selective detection of nitro explosives by a luminescent metal-organic framework. *Angew. Chem.* 52 (10), 2881–2885.
- Pramanik, S., Zheng, C., Zhang, X., Emge, T.J., Li, J., 2011. New microporous metal-organic framework demonstrating unique selectivity for detection of high explosives and aromatic compounds. *J. Am. Chem. Soc.* 133, 4153–4155.
- Shen, L., Liang, S., Wu, W., Liang, R., Wu, L., 2013. CdS-decorated UiO-66(NH₂) nanocomposites fabricated by a facile photodeposition process: An efficient and stable visible-light-driven photocatalyst for selective oxidation of alcohols. *J. Mater. Chem. A* 1, 11473–11482.
- Silva, C.G., Luz, I., Llabrés I Xamena, F.X., Corma, A., García, H., 2010. Water stable Zr-Benzenedicarboxylate metal-organic frameworks as photocatalysts for hydrogen generation. *Chem. Eur. J.* 16, 11133–11138.
- Sonowal, K., Nandal, N., Basyach, P., Kalita, L., Jain, S.L., Saikia, L., 2022. Photocatalytic reduction of CO₂ to methanol using Zr(IV)-based MOF composite with g-C₃N₄ quantum dots under visible light irradiation. *J. CO₂ Util.* 57, 101905.
- Tang, Q., Liu, S., Liu, Y., Miao, J., Li, S., Zhang, L., et al., 2013. Cation sensing by a luminescent metal-organic framework with multiple Lewis basic sites. *Inorg. Chem.* 52, 2799–2801.
- Thorat, K.G., Kamble, P., Ray, A.K., Sekar, N., 2015. Novel pyromethene dyes with N-ethyl carbazole at the meso position: a comprehensive photophysical, lasing, photostability and TD-DFT study. *Phys. Chem. Chem. Phys.* 17, 17221–17236.
- Wang, B., Lin, Y., Tan, H., Luo, M., Dai, S., Lu, H., et al., 2018a. One-pot synthesis of N-doped carbon dots by pyrolyzing the gel composed of ethanalamine and 1-carboxyethyl-3-methylimidazolium chloride and their selective fluorescence sensing for Cr(VI) ions. *Analyst* 143, 1906–1915.
- Wang, B., Lv, X.-L., Feng, D., Xie, L.-H., Zhang, J., Li, M., et al., 2016. Highly stable Zr(IV)-based metal-organic frameworks for the detection and removal of antibiotics and organic explosives in water. *J. Am. Chem. Soc.* 138 (19), 6204–6216.
- Wang, B., Yang, Q., Guo, C., Sun, Y., Xie, L.-H., Li, J.-R., 2017a. Stable Zr(IV)-based metal-organic frameworks with predesigned functionalized ligands for highly selective detection of Fe(III) ions in water. *ACS Appl. Mater. Interfaces* 9, 10286–10295.
- Wang, H., Zhu, Q.L., Zou, R., Xu, Q., 2017b. Metal-organic frameworks for energy applications. *Chem* 2 (1), 52–80.
- Wang, R., Dong, X.-Y., Xu, H., Pei, R.-B., Ma, M.-L., Zang, S.-Q., et al., 2014. A super water-stable europium-organic framework: guests inducing low-humidity proton conduction and sensing of metal ions. *Chem. Commun.* 50, 9153.
- Wang, S., Liu, R., Li, C., 2018b. Highly selective and sensitive detection of Hg²⁺ based on Förster resonance energy transfer between CdSe quantum dots and g-C₃N₄ nanosheets. *Nanoscale Res. Lett.* 13 (1), 235.
- Wang, S.T., Zheng, X., Zhang, S.H., Li, G., Xiao, Y., 2021. A study of GUPT-2, a water-stable zinc-based metal-organic framework as a highly selective and sensitive fluorescent sensor in the detection of Al³⁺ and Fe³⁺ ions. *CrystEngComm* 23, 4059–4068.
- Wang, X., Yang, X., Wang, N., Lv, J., Wang, H., Choi, M.M.F., et al., 2018c. Graphitic carbon nitride quantum dots as an “off-on” fluorescent switch for determination of mercury (II) and sulfide. *Microchim. Acta* 185 (10), 471.
- Wu, X.X., Fu, H.R., Han, M.L., Zhou, Z., Ma, L.F., 2017. Tetraphenylethylene immobilized metal-organic frameworks: highly sensitive fluorescent sensor for the detection of Cr₂O₇²⁻ and nitroaromatic explosives. *Cryst. Growth Des.* 17, 6041–6048.
- Wu, Y.P., Tian, J.W., Liu, S., Li, B., Zhao, J., Ma, L.F., et al., 2019. Bi-microporous metal-organic frameworks with cubane [M₄(OH)₄] (M=Ni, Co) clusters and pore-space partition for electrocatalytic methanol oxidation reaction. *Angew. Chem. Int. Ed.* 58, 12185–12189.
- Xia, T., Song, T., Zhang, G., Cui, Y., Yang, Y., Wang, Z., et al., 2016. A Terbium metal-organic framework for highly selective and sensitive luminescence sensing of Hg²⁺ ions in aqueous solution. *Chem. Eur. J.* 22 (51), 18429–18434.
- Xiang, Z., Fang, C., Leng, S., Cao, D., 2014. An amino group functionalized metal-organic framework as a luminescent probe for highly selective sensing of Fe³⁺ ions. *J. Mater. Chem. A* 2, 7662–7665.
- Yu, F., Chen, L., Shen, X., Li, X., Duan, C., 2019. NH₂-UiO-66/g-C₃N₄/CdTe composites for photocatalytic CO₂ reduction under visible light. *APL Mater.* 7, 101101.
- Zhang, X., Dong, H., Sun, X.J., Yang, D.D., Sheng, J.L., Tang, H.L., et al., 2018. Step-by-step improving photocatalytic hydrogen evolution activity of NH₂-UiO-66 by constructing heterojunction and encapsulating carbon nanodots. *ACS Sustain. Chem. Eng.* 6, 11563–11569.
- Zhang, Y., Chen, Z., Liu, X., Dong, Z., Zhang, P., Wang, J., et al., 2020. Efficient SO₂ removal using a microporous metal-organic framework with molecular sieving effect. *Ind. Eng. Chem. Res.* 59, 874–882.

- Zhang, Z., Chen, Z., Xiao, Y., Yi, M., Zheng, X., Xie, M., et al., 2021. Study of the dynamic adsorption and the effect of the presence of different cations and anions on the adsorption of As(V) on GUT-3. *Appl. Organomet. Chem.* 35, e6289.
- Zhao, D., Wan, X., Song, H., Hao, L., Su, Y., Lv, Y., 2014. Metal-organic frameworks (MOFs) combined with ZnO quantum dots as a fluorescent sensing platform for phosphate. *Sens. Actuators B: Chem.* 197, 50–57.
- Zhao, X.-L., Tian, D., Gao, Q., Sun, H.-W., Xu, J., Bu, X.-H., 2015. A chiral lanthanide metal-organic framework for selective sensing of Fe (III) ions. *Dalton Trans* 45, 1040.
- Zhou, J., Yang, Y., Zhang, C.Y., 2013a. A low-temperature solid-phase method to synthesize highly fluorescent carbon nitride dots with tunable emission. *Chem. Commun.* 49, 8605–8607.
- Zhou, X.-H., Li, L., Li, H.-H., Li, A., Yang, T., Huang, W., 2013b. A flexible Eu(III)-based metal-organic framework: turn-off luminescent sensor for the detection of Fe(III) and picric acid. *Dalton Trans.* 42, 12403.
- Zhou, Y., Chen, H.-H., Yan, B., 2014. An Eu³⁺ post-functionalized nanosized metal-organic framework for cation exchange-based Fe³⁺-sensing in an aqueous environment. *J. Mater. Chem. A* 2, 13691–13697.
- Zhu, J., Xiao, P., Li, H., Carabineiro, S.A.C., 2014. Graphitic carbon nitride: synthesis, properties, and applications in catalysis. *ACS Appl. Mater. Interfaces* 6 (19), 16449–16465.